Nanoscale

COMMUNICATION

View Article Online
View Journal | View Issue

Cite this: *Nanoscale*, 2015, **7**, 9443

Received 22nd March 2015,
Accepted 20th April 2015

DOI: 10.1039/c5nr01820j

www.rsc.org/nanoscale

Thiols as interfacial modifiers to enhance the performance and stability of perovskite solar cells†

Jing Cao,[a] Jun Yin,[a,b] Shangfu Yuan,[a] Yun Zhao,[a] Jing Li[b] and Nanfeng Zheng*[a]

Modifying the interfaces of $CH_3NH_3PbI_3$ with TiO_2 and hole transport layers using two different types of thiols leads to enhanced performance and stability of perovskite solar cells. The incorporation of HOOC–Ph–SH at the TiO_2/perovskite interface facilitates electron transfer from perovskite to TiO_2 and also alters the morphology of perovskite crystal growth to increase the power conversion efficiency. The modification of pentafluorobenzenethiol at the perovskite/hole transport layer interface improves the stability.

Depletion of fossil fuels has led to considerable development in many areas related to photovoltaic cells based on earth-abundant materials. Only within several years, perovskite solar cells (PSSCs) are emerging as one of the most promising candidates for the next generation of cost-effective solar cells with high efficiency.[1–7] Interfacial engineering over the interfaces of the organometal trihalide perovskite layer with the hole and electron extracting layers has been demonstrated to be critical for optimizing the overall performance of PSSCs. With respect to $CH_3NH_3PbI_3$, the TiO_2/Spiro-OMeTAD couple with good optical transparency and perfect band alignment has become one of the most successful interfacial combinations.[2–6,8–12] As for PSSCs based on the mesoporous TiO_2, the efficient contact of the interface between porous titania and perovskite is of paramount importance for their performance as well.

In conventional dye-sensitized solar cells (DSSCs), organic dyes bearing the anchoring groups, such as carboxylic acid moieties, can bind onto the TiO_2 surface to facilitate the electron injection, improving the efficiency of DSSCs.[13–15] With this motivation, organic $HOOCRNH_3^+I^-$ anchor molecules,[16] silane self-assembled monolayers[17] and 3-aminopropanoic acid SAM onto the sol–gel ZnO[18] have also been successfully introduced at the TiO_2/perovskite interface to optimize the overall performance of PSSCs. In most of these studies, alkyl chains are typically present between the binding sites of the anchor molecules involved. It has been well documented that the π-electron acceptors readily facilitate the better electron transfer in DSSCs.[19–21] In this context, we have proposed that the interfacial modification of the TiO_2/$CH_3NH_3PbI_3$ interface with carboxylic acid–thiol ligands (HOOC–Ph–SH) containing a π-electron unit would provide an effective route to improve the conversion efficiency of PSSCs.

Moreover, the poor long-term stability, in particular, when subjected to environmental stress such as light-induced heat and moisture, is the main challenging issue for the commercialization of PSSCs. To address this issue, various strategies, such as controlling the crystallization process of perovskite film,[22–24] introducing the insulating polymer onto the perovskite film[25] and replacing the classic Spiro-OMeTAD with other hole-transports,[26–28] have been investigated. However, the inherent vulnerability of methyl-ammonium lead halide lies in the highly hygroscopic methyl-ammonium cations. Moisture easily breakdowns the structure of methylammonium lead halide.[25] In this work, we also report the use of hydrophobic thiols to enhance the stability of the PSSCs. Thiols containing highly hydrophobic motifs (*e.g.*, $HS–C_6F_5$) were used to cover the perovskite surface by Pb–S coordination (Fig. 1), creating a fully hydrophobic molecular layer to inhibit the intrusion of water molecules into the perovskite film. Such a simple treatment led to much enhanced stability of PSSCs in air and under AM 1.5 G solar light illumination as well.

In this work, the entire fabrication procedure of perovskite solar devices was carried out in open air at a common relative humidity of 45%. As shown in Fig. 1a, the fabricated device adopted the commonly used mesoporous configuration, with thiol-modifications at the interfaces of mesoporous-TiO_2/perovskite and perovskite/Spiro-OMeTAD as well. In a typical procedure, a compact titania layer was deposited on a FTO (fluorine doped tin oxide) conducting glass substrate, which

[a]*State Key Laboratory for Physical Chemistry of Solid Surfaces, Collaborative Innovation Center of Chemistry for Energy Materials, Engineering Research Center for Nano-Preparation Technology of Fujian Province, and Department of Chemistry, College of Chemistry and Chemical Engineering, Xiamen University, Xiamen 361005, China. E-mail: nfzheng@xmu.edu.cn; Fax: +86-592-2183047*

[b]*Pen-Tung Sah Institute of Micro-NanoScience and Technology, Xiamen University, Xiamen 361005, China*

†Electronic supplementary information (ESI) available: Details of the XRD, UV-vis spectra, cross-sectional SEM images and the EQE spectra of the cells. See DOI: 10.1039/c5nr01820j

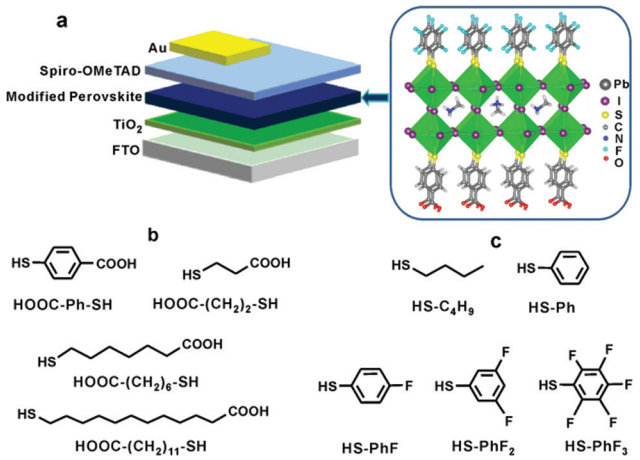

Fig. 1 (a) The schematic structure of the perovskite solar cell modified by HOOC–R–SH and HS–R′ whose molecular structures are shown in (b) and (c), respectively.

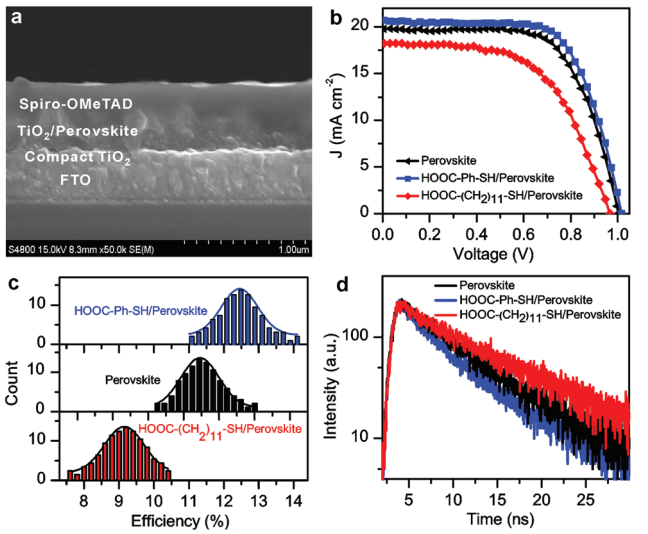

Fig. 2 Cross-sectional SEM image of the device of FTO/TiO_2/HOOC–Ph–SH/perovskite/HS–PhF_5/Spiro-OMeTAD (a). The best *I*–*V* characteristics (b), comparison of the performance distributions of 100 individual devices (c), and the transient PL spectra (d) of perovskite and HOOC–R–SH-based perovskite cells.

was followed by the deposition of a mesoporous TiO_2 layer of 200 nm thickness to enhance electron extraction and transport. Our idea of introducing ligands bearing both carboxylic acid and thiol groups (HOOC–Ph–SH as presented in Fig. 1b) at the interface between porous titania and perovskite layers was to enhance their contact, thus enhancing the electron transfer. Experimentally, the as-obtained TiO_2 mesoporous films were treated with HOOC–R–SH before the deposition of the perovskite layer. The deposited perovskite film was then treated with thiols having hydrophobic groups (HS–R′, as shown in Fig. 1c) to create a hydrophobic molecular layer. The main purpose of such a layer is to block the entrance of water molecules into the perovskite film, thus enhancing its stability against humidity. Finally, a layer of p-type organic hole-conductor Spiro-OMeTAD and the gold cathode were deposited on the top to complete the fabrication. The detailed procedures are given in the ESI.† The structures of the fabricated perovskite devices were characterized by XRD (Fig. S1†), UV-Vis (Fig. S2†) and SEM (Fig. 2a, S3 and S4†). All these data indicated that the perovskite structures were well-formed in all of the fabricated solar cells.[29,30]

To confirm the successful anchoring of carboxylic acid–thiol between mesoporous TiO_2 and perovskite, FTIR spectra of films during the fabrication of devices were recorded (Fig. S5†). In the case where HOOC–Ph–SH was used as a molecular solder for the mesoporous TiO_2 and perovskite, the HOOC–Ph–SH/perovskite film displayed an absorption peak at 1697 cm^{-1} which can be assigned to COO stretching. The disappearance of the absorption peak at 2581 cm^{-1} and the appearance of the absorption peak at 435 cm^{-1} suggests the coordination of SH-groups to Pb on the perovskite. The peak at 435 cm^{-1} can be assigned to the Pb–S coordination-function.[31] These results demonstrated the successful anchoring of carboxylic acid–thiol between TiO_2 and perovskite with –COOH bound to TiO_2 and –SH bound to Pb on the perovskite.

In order to demonstrate the effect of carboxylic acid–thiol linkers on the electron transfer at the TiO_2/perovskite interface, the overall performance of the FTO/TiO_2/HOOC–R–SH/perovskite/Spiro-OMeTAD devices (Fig. 2a) was measured under AM 1.5, 100 mW cm^{-2} light illumination. The incident photon-to-current conversion efficiency spectra (IPCE) of the cells spanned from the UV region to 800 nm (Fig. S6†), matching well with their UV-Vis absorption spectra (Fig. S2†). As illustrated in Fig. 2b, c, S7 and Table S1,† the incorporation of HOOC–Ph–SH at the TiO_2/perovskite interface did enhance the overall performance of the solar cells. The best efficiency of 14.1% was observed from the solar cells fabricated with HOOC–Ph–SH. Measurements over 100 fabricated cells gave an average efficiency of 12.4 ± 1.8%. In comparison, 100 devices fabricated without HOOC–Ph–SH offered an average efficiency of 11.6 ± 1.6% with the best device reaching a power-conversion efficiency of 13.2%. The best device was fabricated with the HOOC–Ph–SH ligand bearing the π-electron motif with the short-circuit current density (J_{sc}), open-circuit voltage (V_{oc}) and fill factor (FF) being 20.66 mA cm^{-2}, 1.02 V and 0.67, respectively.

To further confirm the enhanced electron transfer in the HOOC–R–SH modified perovskite solar cells, the transient photoluminescence (PL) measurements were also carried out using the steady state and time-resolved fluorescence method (Fig. 2d). Interestingly, compared to the perovskite-only film with a decay time of τ = 9.3 ns, the film with the HOOC–Ph–SH modification exhibited a relatively short transient decay time of 7.6 ns. While, the film with HOOC–$(CH_2)_{11}$–SH had a longer decay time of 11.9 ns. The longer lifetime for the HOOC–$(CH_2)_{11}$–SH modified cell may have been caused by the weak electron transfer ability due to the presence of the long alkyl chain between –COOH and –SH motifs, therefore leading to a

faster electron recombination. The relatively short lifetime for the cells having HOOC–Ph–SH bound at the interface between the TiO_2 and $CH_3NH_3PbI_3$ layers suggested a π-electron transport-method to retard the charge recombination, resulting in an overall enhanced photovoltaic performance. It should also be noted that the introduction of HOO–R–SH binders altered the growth behavior of perovskites. As shown in the top-view SEM images of the as-prepared HOOC–R–SH modified perovskite films (Fig. 3), the $CH_3NH_3PbI_3$ nanocrystals supported on the TiO_2 are evidently larger in size, compared to that of the perovskite-only sample. At this point, it is still unclear how the HOOC–R–SH modification promotes the electron transfer from perovskite to TiO_2. More work is still needed to determine whether the overall improved efficiency originated from the electronic effect, the morphological effect or both.

The long-term stability is among the biggest remaining challenges in perovskite solar cells. Water, which is a Lewis base, readily combines with $CH_3NH_3PbI_3$ and removes the ammonium from the perovskite structure, leading to an easy breakdown of the perovskite framework. While the thiol modification at the TiO_2/perovskite interface helped to promote the electron transfer to some extent, such a modification did not enhance cells' stability (Fig. S8†). Owing to the strong coordination of thiol on Pb^{2+}, employing hydrophobic thiols to create a molecular protection layer on perovskite might be an effective method to stabilize perovskite solar cells against humidity. Following this idea, we applied a series of HS–R′ ligands (Fig. 1c) to decorate the perovskite films before the deposition of Spiro-OMeTAD. With such a modification, the surface of the perovskite nanocrystallites was slightly eroded (Fig. 3d). The successful modification of thiol on the perovskite surface was confirmed by the disappearance of the IR absorption peak of –SH at 2581 cm^{-1} and the absorption peak of Pb–S at 435 cm^{-1} (Fig. S5†).

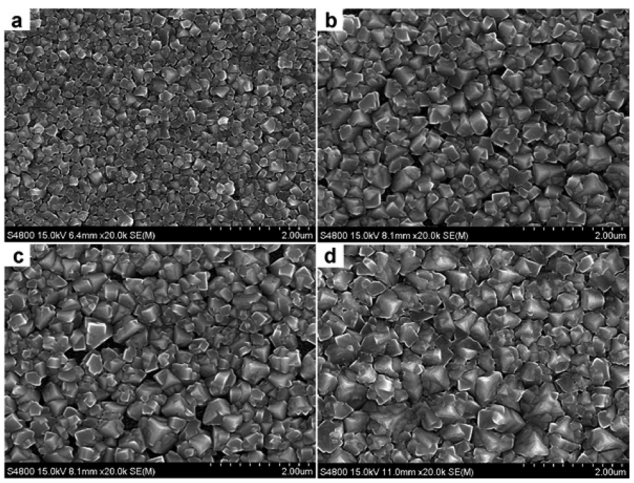

Fig. 3 SEM images showing the surfaces of (a) TiO_2/perovskite, (b) TiO_2/HOOC–$(CH_2)_{11}$–SH/perovskite, (c) TiO_2/HOOC–Ph–SH/perovskite, and (d) TiO_2/HOOC–Ph–SH/perovskite/HS–PhF_5 deposited on FTO glasses.

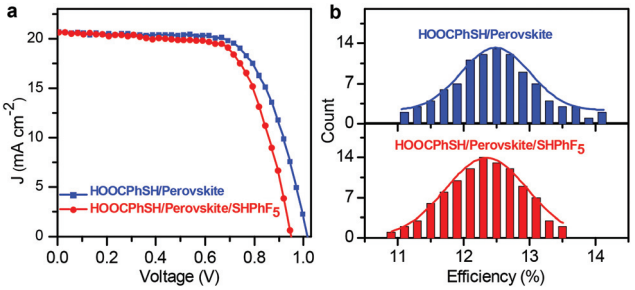

Fig. 4 (a) The *I–V* characteristics of the best cells and (b) the performance distributions of 100 individual devices of HOOC–Ph–SH/perovskite and HOOC–Ph–SH/perovskite/HS–R′.

As shown in the *I–V* and IPCE curves of the most-efficient cells (Fig. 4, S9 and S10†), the features of photocurrent responses in the range from 300 nm to 800 nm with the maximum efficiency of over 80% roughly resemble their respective absorption spectra (Fig. S2†). The modification of hydrophobic thiols on perovskite did not alter the average performance of the cells (Fig. 4b and S10†), although the best efficiencies slightly decreased. Compared to the cells without the HS–R′ modification, the cells with the modification exhibited poorly fill factors and low voltages, which might be explained by the fact that the surface modification of thiols on the perovskite surface retarded the efficient contact between the perovskite and hole transport layers.

Without causing much deleterious effects to the cells' overall performance, the surface modification of perovskite by "water-resistant" HS–R′ ligands offers an effective protection method to improve the stability of perovskite solar cells. As shown in Fig. 5a, when stored in air at room temperature with a humidity of about 45%, the perovskite solar cells with the encapsulation of HS–PhF_5 showed no obvious color change in 8 days. In comparison, in the same period, the cells without the thiol encapsulation decayed to a great extent and the color faded from dark to yellow. Accordingly, the HS–R′ modification experienced a marked increase in stability, especially the HS–PhF_5 ligand bearing hydrophobic fluorine units (Fig. 5b and S11†). The devices with the HS–PhF_5 modification retained over 80% of their original efficiency after 10-day storage in air with a relative humidity of ~45%. In contrast, under the same storage conditions, the cells with thiol modification lost ~80% of their efficiency after 10 days. The cells with thiol modification exhibited much enhanced stability under illumination in humid air as well. As under illumination at AM 1.5 G (Fig. 5c and S12†), the cells without thiol modification lost 50% of their activities within 50 min. In comparison, the time for the cells with the HS–PhF_5 to lose 50% of their original efficiencies was extended beyond 200 min. These results nicely demonstrate that the deposition of hydrophobic thiol at the interface between perovskite and hole transport layers can efficiently inhibit the escape of methylammonium and entrance of water molecules, providing an effective molecular sealing approach to enhance the stability of perovskite solar cells.

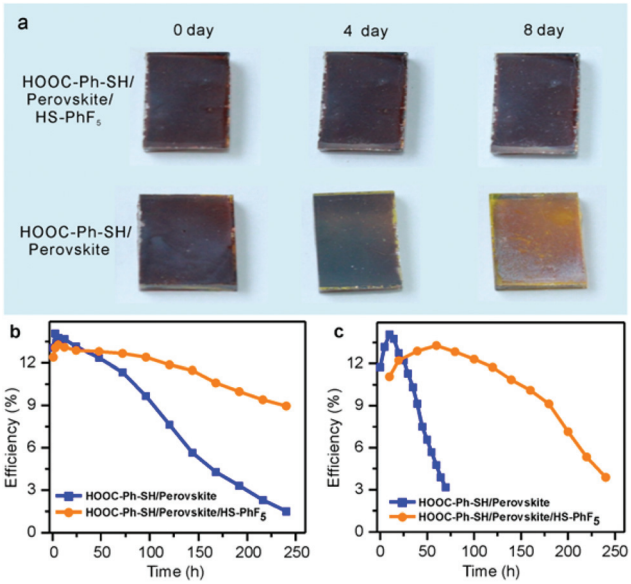

Fig. 5 The color variation of HOOC–Ph–SH/perovskite/Spiro-OMeTAD and HOOC–Ph–SH/perovskite/HS–R′/Spiro-OMeTAD films stored in air at room temperature with a humidity of about 45% (a). The efficiency variation of the devices stored in air at room temperature with the humidity of 45% (b) and under illumination at AM 1.5 G (c).

Conclusions

In conclusion, an effective interfacial modification route using thiols has been developed to improve both performance and stability of perovskite solar cells. The chemical modification at the TiO_2/perovskite interface by HOOC–Ph–SH facilitated the growth of bigger perovskite crystallites and enhanced the transfer of photo-generated electrons from perovskite to TiO_2 as well. With such a modification, the best photon-to-current conversion efficiency of 14.1% was observed for the perovskite solar cells fabricated under ambient conditions. Furthermore, modifying the perovskite/Spiro-OMeTAD interface with hydrophobic thiols, especially HS–PhF_5 remarkably improved the stability of PSSCs in air or under AM 1.5 G solar light illumination. The developed interfacial modification approach should be effective to enhance both conversion efficiency and stability of perovskites having other architectures.

Acknowledgements

We thank the MOST of China (2011CB932403) and the NSFC of China (21420102001, 21131005, 21390390) for financial support.

Notes and references

1 J.-H. Im, C.-R. Lee, J.-W. Lee, S.-W. Park and N.-G. Park, *Nanoscale*, 2011, **3**, 4088–4093.
2 H.-S. Kim, C.-R. Lee, J.-H. Im, K.-B. Lee, T. Moehl, A. Marchioro, S.-J. Moon, R. Humphry-Baker, J.-H. Yum, J. E. Moser, M. Grätzel and N.-G. Park, *Sci. Rep.*, 2012, **2**, 1–7.
3 A. Kojima, K. Teshima, Y. Shirai and T. Miyasaka, *J. Am. Chem. Soc.*, 2009, **131**, 6050–6051.
4 M. M. Lee, J. Teuscher, T. Miyasaka, T. N. Murakami and H. J. Snaith, *Science*, 2012, **338**, 643–647.
5 M. Liu, M. B. Johnston and H. J. Snaith, *Nature*, 2013, **501**, 395–398.
6 W. Nie, H. Tsai, R. Asadpour, J.-C. Blancon, A. J. Neukirch, G. Gupta, J. J. Crochet, M. Chhowalla, S. Tretiak and M. A. Alam, *Science*, 2015, **347**, 522–525.
7 H. Zhou, Q. Chen, G. Li, S. Luo, T.-b. Song, H.-S. Duan, Z. Hong, J. You, Y. Liu and Y. Yang, *Science*, 2014, **345**, 542–546.
8 S. Dharani, H. K. Mulmudi, N. Yantara, P. T. Thu Trang, N. G. Park, M. Grätzel, S. Mhaisalkar, N. Mathews and P. P. Boix, *Nanoscale*, 2014, **6**, 1675–1679.
9 M. A. Green, A. Ho-Baillie and H. J. Snaith, *Nat. Photonics*, 2014, **8**, 506–514.
10 S. Kazim, M. K. Nazeeruddin, M. Grätzel and S. Ahmad, *Angew. Chem., Int. Ed.*, 2014, **53**, 2812–2824.
11 P. Qin, A. L. Domanski, A. K. Chandiran, R. Berger, H. J. Butt, M. I. Dar, T. Moehl, N. Tetreault, P. Gao, S. Ahmad, M. K. Nazeeruddin and M. Grätzel, *Nanoscale*, 2014, **6**, 1508–1514.
12 L. Zhu, J. Xiao, J. Shi, J. Wang, S. Lv, Y. Xu, Y. Luo, Y. Xiao, S. Wang, Q. Meng, X. Li and D. Li, *Nano Res.*, 2015, DOI: 10.1007/s12274-12014-10592-y.
13 P. Wang, S. M. Zakeeruddin, J. E. Moser, M. K. Nazeeruddin, T. Sekiguchi and M. Grätzel, *Nat. Mater.*, 2003, **2**, 402–407.
14 Z. Yao, M. Zhang, H. Wu, L. Yang, R. Li and P. Wang, *J. Am. Chem. Soc.*, 2015, **137**, 3799–3802.
15 A. Yella, H.-W. Lee, H. N. Tsao, C. Yi, A. K. Chandiran, M. K. Nazeeruddin, E. W.-G. Diau, C.-Y. Yeh, S. M. Zakeeruddin and G. Michael, *Science*, 2011, **334**, 629–633.
16 Y. Ogomi, A. Morita, S. Tsukamoto, T. Saitho, Q. Shen, T. Toyoda, K. Yoshino, S. S. Pandey, T. Ma and S. Hayase, *J. Phys. Chem. C*, 2014, **118**, 16651–16659.
17 L. Liu, A. Mei, T. Liu, P. Jiang, Y. Sheng, L. Zhang and H. Han, *J. Am. Chem. Soc.*, 2015, **137**, 1790–1793.
18 L. Zuo, Z. Gu, T. Ye, W. Fu, G. Wu, H. Li and H. Chen, *J. Am. Chem. Soc.*, 2015, **137**, 2674–2679.
19 W. M. Campbell, A. K. Burrell, D. L. Officer and K. W. Jolley, *Coord. Chem. Rev.*, 2004, **248**, 1363–1379.
20 S. Fukuzumi and T. Kojima, *J. Mater. Chem.*, 2008, **18**, 1427.
21 Q. Wang, W. M. Campbell, E. E. Bonfantani, K. W. Jolley, D. L. Officer, P. J. Walsh, K. Gordon, R. Humphry-Baker, M. K. Nazeeruddin and M. Grätzel, *J. Phys. Chem. B*, 2005, **109**, 15397–15409.
22 S. Bai, Z. Wu, X. Wu, Y. Jin, N. Zhao, Z. Chen, Q. Mei, X. Wang, Z. Ye, T. Song, R. Liu, S.-t. Lee and B. Sun, *Nano Res.*, 2014, **7**, 1749–1758.
23 L. Chen, F. Tang, Y. Wang, S. Gao, W. Cao, J. Cai and L. Chen, *Nano Res.*, 2015, **8**, 263–270.

24 F. X. Xie, D. Zhang, H. Su, X. Ren, K. S. Wong, M. Grätzel and W. C. H. Choy, *ACS Nano*, 2015, **1**, 639–646.
25 S. N. Habisreutinger, T. Leijtens, G. E. Eperon, S. D. Stranks, R. J. Nicholas and H. J. Snaith, *Nano Lett.*, 2014, **14**, 5561–5568.
26 S. Lv, L. Han, J. Xiao, L. Zhu, J. Shi, H. Wei, Y. Xu, J. Dong, X. Xu, D. Li, S. Wang, Y. Luo, Q. Meng and X. Li, *Chem. Commun.*, 2014, **50**, 6931–6934.
27 A. Mei, X. Li, L. Liu, Z. Ku, T. Liu, Y. Rong, M. Xu, M. Hu, J. Chen and Y. Yang, *Science*, 2014, **345**, 295–298.
28 Z. Wu, S. Bai, J. Xiang, Z. Yuan, Y. Yang, W. Cui, X. Gao, Z. Liu, Y. Jin and B. Sun, *Nanoscale*, 2014, **6**, 10505–10510.
29 J. Burschka, N. Pellet, S.-J. Moon, R. Humphry-Baker, P. Gao, M. K. Nazeeruddin and M. Grätzel, *Nature*, 2013, **499**, 316–319.
30 Y. Wu, A. Islam, X. Yang, C. Qin, J. Liu, K. Zhang, W. Peng and L. Han, *Energy Environ. Sci.*, 2014, **7**, 2934–2938.
31 R. A. Nyquist, C. L. Putzig, R. O. Kagel and M. A. Leugers, *Infrared spectra of inorganic compounds*, Academic Press, New York, 1971.